RSC Advances

PAPER

View Article Online
View Journal | View Issue



Cite this: *RSC Adv.*, 2021, **11**, 29385

# *N*-Aryl iminochromenes inhibit cyclooxygenase enzymes *via* π–π stacking interactions and present a novel class of anti-inflammatory drugs†

Ha Thi Nguyen,[ab] Thien-Y. Vu,[c] A. Vijay Kumar,[d] Vo Nguyen Huy Hoang,[c] Pham Thi Ngoc My,[c] Prashant S. Mandal[d] and Vinay Bharadwaj Tatipamula *[ab]

Cyclooxygenase enzymes (COX1/2) have been widely studied and noted for their role in the biosynthesis of inflammation-induced proteins, prostaglandins and thromboxane. Multiple anti-inflammatory drugs have been developed to target these two enzymes, but most of them appeared to have notable adverse effects, especially on the cardiovascular system and lower gastrointestinal tract, suggesting an urgent need for new potent anti-inflammatory drugs. In this study, we screened twenty-two previously synthesized *N*-aryl iminochromenes (NAIs) for their anti-inflammatory activity by performing COX-1/2 inhibitory assays. Five compounds (**1**, **10**, **14**, **15**, and **20**) that gave the best *in vitro* anti-inflammatory results were subjected to an *in vivo* anti-inflammatory assay using the formalin-induced hind rat paw oedema method, followed by *in silico* studies using indomethacin and celecoxib as standard drugs. Among them, compound **10** stood out as the best candidate, and the percentage reduction in paw oedema at the dose of 20 mg $kg^{-1}$ body weight was found to be substantially higher with compound **10** than that with indomethacin. This is mostly due to the excellent suitability of the chromene-phenyl scaffold with a highly concentrated area of aromatic residues, which produced good π–π stacking interactions. Taken together, this study strongly suggests compound **10** as a potential candidate for anti-inflammatory drug research.

Received 7th June 2021
Accepted 15th August 2021

DOI: 10.1039/d1ra04407a

rsc.li/rsc-advances



## Introduction

Inflammation is a normal response of the immune system against injury to neutralize the invading pathogens and repair the injured tissues, thereby promoting wound healing.[1] Although inflammation is a self-limiting process, it can become chronic and cause several other serious complications,[2,3] including cancer,[4] atherosclerosis,[5] Alzheimer's disease,[6] and rheumatoid arthritis.[7] Historically, non-steroidal anti-inflammatory drugs (NSAIDs), including organic acids and non-acidic compounds, have been largely used in the treatment of inflammation.[8] Indomethacin (a potent NSAID) is a COX-1/2 inhibitor that has been widely used as an anti-inflammatory, antipyretic, and analgesic agent for decades with several reported severe adverse effects on the GI tract.[9,10]

In 1990s, several first *in vivo* studies involving anti-inflammatory agents were investigated, resulting in the successful discovery of anti-inflammatory drugs with fewer side effects on the gastrointestinal (GI) tract commonly caused by NSAIDs.[11] Thereafter, numerous molecular and cellular pharmacological studies have been carried out, leading to the identification of the cyclooxygenase-1/2 (COX-1/2) enzymes. These enzymes are responsible for the physiological production of prostaglandins (PGs) and thromboxane (TXA2), which primarily cause inflammation.[11] COX-1 plays a crucial role in the regulation of GI, renal, and vascular functions, while COX-2 regulates cytokines, endotoxins, and mitogens in inflammation, pain, and fever.[12,13] These findings served as the basis for the development of selective COX-2 inhibitor drugs, such as celecoxib and rofecoxib. However, these drugs appeared to have serious adverse effects on the cardiovascular[14] and lower GI[15] systems. To address these issues, many attempts have been made in the last decade to develop new natural product-based/like-anti-inflammatory drugs with fewer and milder adverse effects.[16–20]

Noticeably, "chromene"-based compounds have drawn much attention from researchers and are considered as an important source for developing new anti-inflammation drugs.[19,21] Different series of chromene analogues have been reported to have pharmacological activities, including anti-inflammatory, anticancer, and antimicrobial actions.[21,22] For decades, various 2*H*-chromene-containing scaffolds like

[a]*Institute of Research and Development, Duy Tan University, Da Nang 550000, Vietnam. E-mail: vinaybharadwajtatipamula@duytan.edu.vn*
[b]*Faculty of Medicine, Duy Tan University, Da Nang 550000, Vietnam*
[c]*Faculty of Pharmacy, Ton Duc Thang University, Ho Chi Minh City 700000, Vietnam*
[d]*Department of Chemistry, Institute of Chemical Technology, Mumbai 400019, India*
† Electronic supplementary information (ESI) available. See DOI: 10.1039/d1ra04407a

coumarins and 2-imino/oxo-2*H*-1-benzopyran-3-carboxamides have been well-acknowledged for their anti-inflammatory properties.[23–25] Further, the structure–activity relationship (SAR) of 2*H*-chromene at various positions, including C-3, C-6, and C-7, have been studied.[24] Markedly, *via* a cross-coupling strategy, our group has successfully synthesized twenty-two *N*-aryl iminochromenes (NAIs),[26] which belong to a class of novel 2*H*-chromene ring-containing molecules with different *N*-arylimino substituents vicinal to the oxygen (Fig. 1).

In this study, we aimed to investigate the anti-inflammatory activities of these NAIs by performing an *in vitro* anti-inflammatory assay against COX-1 and COX-2 enzymes, followed by an *in vivo* anti-inflammatory assay using the formalin-induced hind rat paw oedema method and *in silico* studies using indomethacin as the reference drug.

## Results and discussion

### COX-1 inhibitory assay

The COX-1 inhibitory assay results revealed that 20 out of 22 tested compounds had better inhibition capacity against the COX-1 enzyme (with lower $IC_{50}$ values) compared with that of indomethacin (15.4 ± 0.6 nM). Among these, compounds **10**, **15**, **5**, **14**, **16**, **1**, **20** and **2** exhibited the highest inhibition

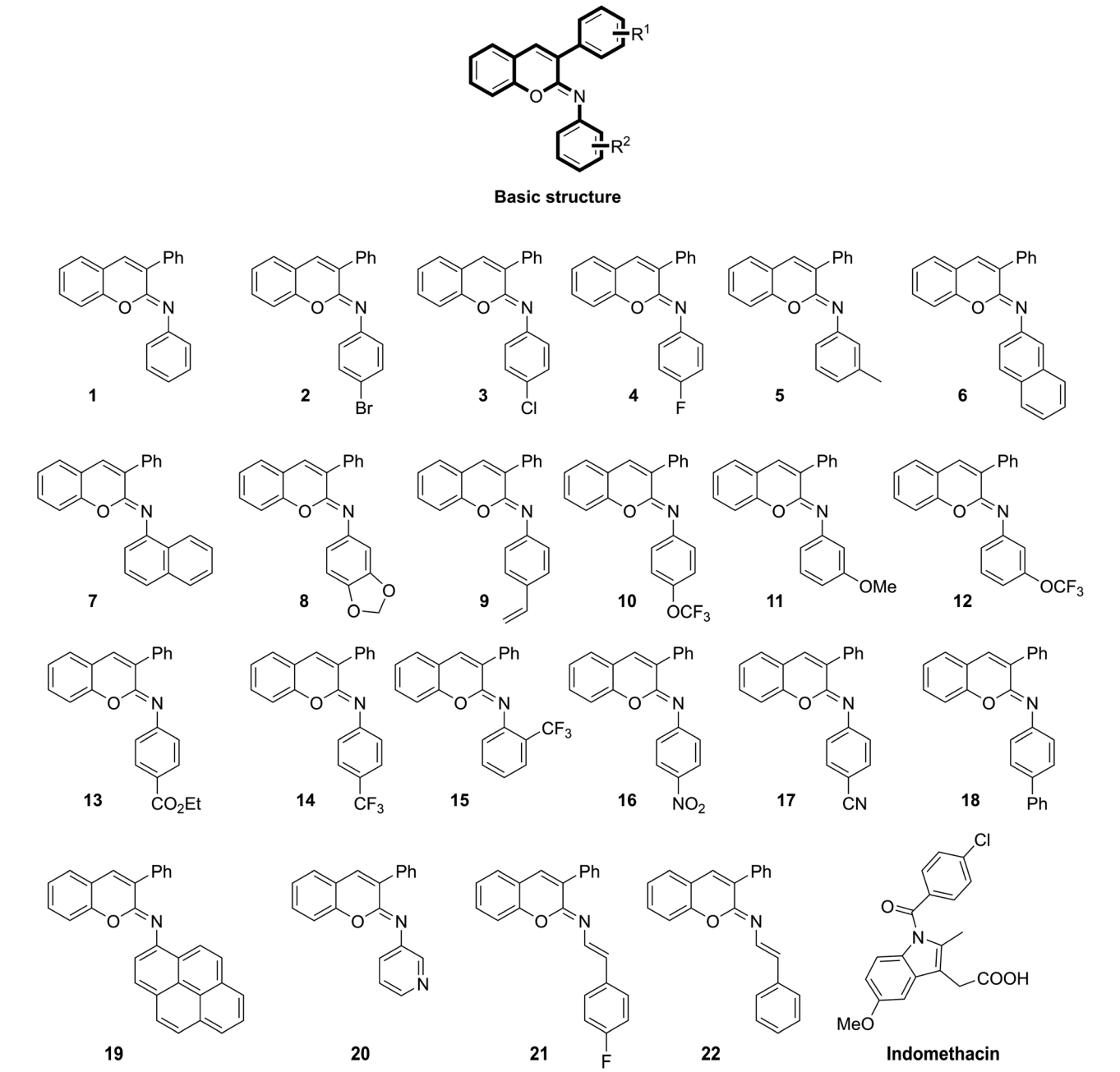


Fig. 1 Chemical structures of the previously reported *N*-aryl iminochromene derivatives[26] and the standard drug indomethacin.

Table 1 *In vitro* bioassay results of the *N*-aryl iminochromene derivatives

| Compound | Half-maximal inhibitory concentration ($IC_{50}$) values[a] (nM) | |
|---|---|---|
| | Cyclooxygenase-1 | Cyclooxygenase-2 |
| **1** | 9.0 ± 0.5*** | 9.7 ± 1.2* |
| **2** | 10.1 ± 0.7*** | 12.4 ± 0.4 |
| **3** | 10.9 ± 0.5** | 8.5 ± 0.2** |
| **4** | 11.8 ± 0.4 | 11.1 ± 0.5 |
| **5** | 8.4 ± 0.3*** | 10.2 ± 1.1 |
| **6** | 20.7 ± 0.4 | 16.2 ± 0.3 |
| **7** | 12.6 ± 1.3 | 8.3 ± 0.7*** |
| **8** | 12.3 ± 0.6 | 14.0 ± 0.1 |
| **9** | 13.7 ± 0.5 | 12.7 ± 0.5 |
| **10** | 7.3 ± 0.5*** | 9.5 ± 0.5* |
| **11** | 16.0 ± 0.4 | 8.7 ± 0.6** |
| **12** | 18.4 ± 0.6 | 11.3 ± 0.9 |
| **13** | 14.4 ± 1.0 | 10.0 ± 1.2* |
| **14** | 8.7 ± 0.8*** | 8.7 ± 0.7** |
| **15** | 7.4 ± 0.5*** | 7.8 ± 0.6*** |
| **16** | 9.7 ± 0.7*** | 13.1 ± 0.9 |
| **17** | 19.5 ± 0.9 | 19.2 ± 0.6 |
| **18** | 20.6 ± 1.1 | 11.3 ± 0.5 |
| **19** | 9.9 ± 0.9*** | 10.6 ± 1.7 |
| **20** | 9.7 ± 1.2*** | 9.6 ± 1.0* |
| **21** | 11.5 ± 0.8* | 14.0 ± 0.6 |
| **22** | 15.1 ± 0.2 | 18.3 ± 0.9 |
| Indomethacin | 15.4 ± 0.6 | 14.7 ± 1.7 |
| Celecoxib | — | 7.1 ± 0.5 |

[a] Values are presented as the mean ± standard deviation of three individual experiments ($n = 3$). Statistical analyses were done by one-way analysis of variance followed by Tukey's test; *$p < 0.05$, **$p < 0.001$ and ***$p < 0.0001$ indicate a significant reduction compared with that of the standard drug, indomethacin.

capacity with $IC_{50}$ values in the range of 7.3 ± 0.5 to 10.1 ± 0.7 nM, which were significantly lower than that of indomethacin ($p < 0.001$) (Table 1).

### COX-2 inhibitory assay

Similarly, the COX-2 inhibitory assay outcomes pointed out that 18 out of 22 compounds in this study displayed higher inhibition ability toward COX-2 than indomethacin ($IC_{50}$: 14.7 ± 1.7 nM). Of these, compounds **15**, **7**, **3**, **14**, **11**, **10**, **20** and **1** possessed the best inhibition capacity against COX-2 (with the $IC_{50}$ values varying from 7.8 ± 0.6 to 9.7 ± 1.2 nM), which were significantly lower than that of indomethacin and marginally higher than celecoxib (7.1 ± 0.5) (Table 1).

### Acute toxicity studies

Compound **1** was used to evaluate the median lethal dose ($LD_{50}$) in male albino rats using the oral acute toxic class method.[27] Accordingly, no clinical signs were observed in the male rats, and the $LD_{50}$ of compound **1** was found to be above 200 mg $kg^{-1}$ body weight (b.w), and the low and high dosages were respectively fixed at 10 and 20 mg $kg^{-1}$ b.w.

### *In vivo* studies

The best five compounds, namely **1**, **10**, **14**, **15** and **20**, which had the highest protection capacity against both COX-1 and COX-2 enzymes *in vitro*, were selected for further *in vivo* studies using the standard protocol of formalin-induced rat paw oedema by plethysmography, as described previously.[28] The effects of these compounds and the standard drugs (indomethacin and celecoxib) on the rat paw oedema were measured relative to the control (Fig. 2). The results are presented as the percentage reduction of oedema relative to the basal paw volume at two doses: 10 and 20 mg $kg^{-1}$ b.w (Fig. 3). Noticeably, the tested NAIs showed good potency in reducing paw oedema at both tested doses compared with indomethacin and celecoxib (Fig. 3). The paw-inflamed rats dosed with compounds **1**, **10**, **14**, **15** and **20** exhibited a remarkable reduction in paw oedema. Of these, compound **14** presented with the lowest percentage reduction at both low and high doses for all the measured time-points (1, 2 and 4 h) (Fig. 3).

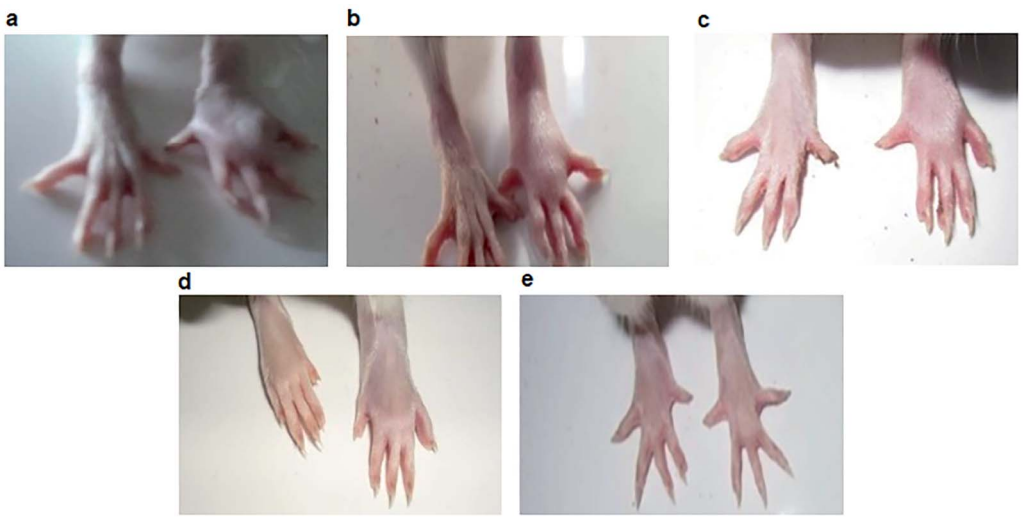


Fig. 2 Paw oedema images of albino rats. (a) Control group; (b) indomethacin-treated group; (c) celecoxib-treated group; (d) compound **10**-treated group; (e) compound **15**-treated group at 20 mg $kg^{-1}$ body weight.

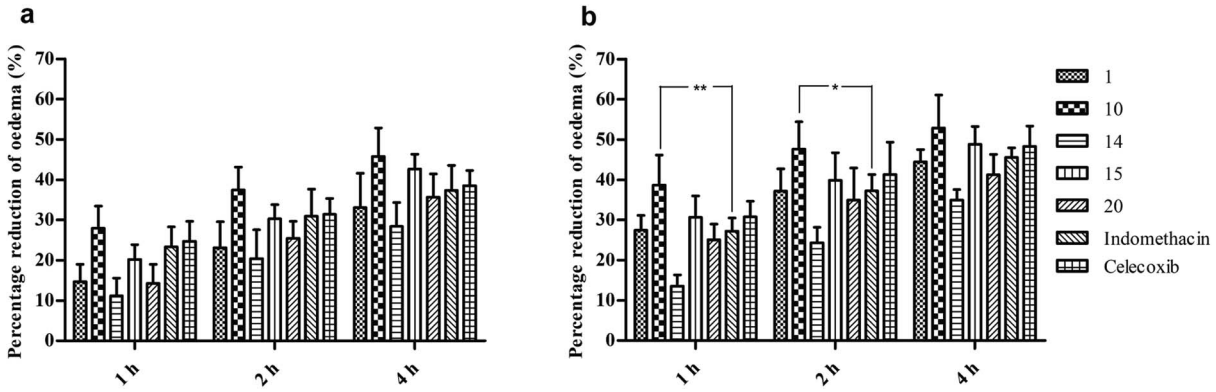


Fig. 3 *In vivo* anti-inflammatory activity of *N*-aryl iminochromenes. (a) The percentage reduction of rat paw oedema at a low dose (10 mg $kg^{-1}$ body weight (b.w)), and (b) the percentage of reduction of rat paw oedema at a high dose (20 mg $kg^{-1}$ b.w) at 1, 2 and 4 h. The data are presented as the mean ± standard error of mean of five biological replicates. The statistical analysis was performed using two-way analysis of variance followed by Bonferroni post-tests. The star (*) mark indicates a significant difference between the two groups with *$p < 0.05$ or **$p < 0.01$.

On the other hand, compounds **10** and **15** were the most effective compounds in reducing paw oedema in the rats. Specifically, treatment with a low dose of compound **10** showed a higher reduction in rat paw oedema at all the three time-points (27.9 ± 2.5, 37.5 ± 2.5, and 45.8 ± 3.2%) compared with those of indomethacin (23.3 ± 2.2, 31.0 ± 3.0, and 37.4 ± 2.8%) and celecoxib (24.7 ± 2.2, 31.4 ± 1.8, and 38.5 ± 1.7) though the differences were not significant (Fig. 3a). At a high dose, the compound **10**-treated group showed potent activity with 38.7 ± 3.4, 47.6 ± 3.1, and 52.9 ± 3.6% reduction in rat paw oedema at 1, 2 and 4 h, respectively. Noticeably, the percentage of paw oedema inhibition in the compound **10**-treated group was significantly higher than that of the indomethacin-treated group at 1 h ($p < 0.01$) and 2 h ($p < 0.05$) after treatment (Fig. 3b). Similarly, compound **15** exhibited a good reduction in paw oedema, and the reduction rates were found to be 20.2 ± 1.7, 30.3 ± 1.6, and 42.7 ± 1.6% for the low dose and 30.7 ± 2.4, 39.9 ± 3.1, and 48.9 ± 2.0% for the high dose at 1, 2 and 4 h, respectively, equivalent to that of the indomethacin and celecoxib (Fig. 3).

### Structure–activity relationship (SAR)

According to the results, most of the tested NAIs were potent against inflammation. From the COX-1/2 inhibitory studies, we explored the SAR of the new class of NAIs that have various substituents at different $\mathbf{R^2}$ positions for their anti-inflammatory activities.

- The synthesis of fluoro-substituted derivatives (like $-CF_3$) at the *ortho* or *para* position of $\mathbf{R^2}$ improved the biological activity.
- Substitution with electron-donating groups (like $-CH_3$) at the *meta* position of $\mathbf{R^2}$ improved the pharmacological activity than did electron-withdrawing groups, such as $-OCF_3$ and $-OCH_3$.
- The placement of electron-withdrawing groups, such as phenyl, nitro, esters, and cyano groups, at the *para* position of $\mathbf{R^2}$ produces less activity.
- The presence of heterocyclic aromatic moieties (like 1,3-benzodioxole and pyridine) in place of $\mathbf{R^2}$ decreased the potency.

Table 2 The MM-GBSA binding free energies estimations (kcal $mol^{-1}$) of the five best ligands and the reference drug indomethacin. The rigid and IFD top 1 poses are the best docking scores for each individual method, while IFD top 2 was selected flexibly among the two best IFD docking scores[a]

| | Cyclooxygenase-1 | | | | | Cyclooxygenase-2 | | | | |
|---|---|---|---|---|---|---|---|---|---|---|
| | MM-GBSA estimation (kcal $mol^{-1}$) | | | | | MM-GBSA estimation (kcal $mol^{-1}$) | | | | |
| Ligands | Rigid | IFD (top 1) | IFD (top 2) | $\Delta G_{exp}$ (kcal $mol^{-1}$) | RMSD of rigid and IFD top 1 | Rigid | IFD (top 1) | IFD (top 2) | $\Delta G_{exp}$ (kcal $mol^{-1}$) | RMSD of rigid and IFD top 1 |
| **1** | −80.6 | −84.3 | −84.3 | −11.0 | 0.1 | −73.7 | −95.0 | −84.7 | −11.0 | 0.2 |
| **10** | −73.8 | −86.2 | −96.6 | −11.2 | 1.0 | −58.2 | −89.0 | −89.0 | −11.0 | 0.4 |
| **14** | −78.5 | −88.0 | −88.0 | −11.1 | 1.2 | −53.6 | −88.7 | −88.7 | −11.1 | 0.9 |
| **15** | −66.2 | −95.6 | −95.6 | −11.2 | 0.6 | −61.5 | −106.9 | −106.9 | −11.1 | 0.6 |
| **20** | −78.4 | −87.9 | −83.1 | −11.0 | 0.1 | −73.6 | −83.1 | −83.1 | −11.0 | 0.5 |
| Indomethacin | −32.3 | −76.2 | −55.2 | −11.0 | 0.4 | −26.4 | −53.9 | −44.6 | −10.8 | 0.9 |
| Celecoxib | — | — | — | — | — | **−37.6** | **−49.8** | **−60.9** | **−11.2** | **0.9** |
| Average | **−68.3** | **−88.1** | **−87.4** | **−11.0** | **0.8** | **−54.9** | **−84.2** | **−84.3** | **−11.0** | **0.7** |

[a] MM-GBSA: molecular mechanics/generalized born surface area; IFD: induced fit docking; RMSD: root-mean-square deviation; $\Delta G_{exp}$: experimental binding free energy.

- The substitution of halogens at the *para* position of $\mathbf{R^2}$ produced activity in the order Br > Cl > F.
- The replacement of the phenyl moiety with styrene at $\mathbf{R^2}$ produced less pharmacological activity than its *para*-fluoro derivative.
- The replacement of the phenyl moiety with polycyclic/bicyclic rings like pyrene/naphthalene at $\mathbf{R^2}$ was found to decrease the biological activity.
- The *para* substitution of a phenyl moiety at $\mathbf{R^2}$ shortened the activity.

### Docking studies

To understand the possible mechanisms of action through which the NAIs inhibit COX-1/2 functions, the five ligands were subjected to molecular modelling. Three numerical values for the Glide rigid docking, induced fit docking (IFD) top 1 and IFD top 2 poses with COX-1 and COX-2 are presented in Table 2.

Firstly, the five studied compounds had good mean experimental binding energies at $-11.0$ kcal mol$^{-1}$ similar to those of indomethacin and celecoxib. This was a typical case where all five compounds were with nearly flat SAR. In other words, even with different substituents on the central scaffold, these compounds still matched the binding sites of the COX-1/2 enzyme, but no key interactions could be generated. Therefore, a correlation between the theoretical and experimental energies has not been performed. This finding, however, highlighted the decisive role of the central scaffolds and suggested the need for further theoretical analyses.

For the COX-1 protein, the theoretically estimated values showed a good correlation ($R^2$) with the experimental results, and the $R^2$ values of rigid docking, IFD top 1 and IFD top 2 were 0.61, 0.14, and 0.84, respectively (Table 2). Generally, due to a higher degree of accuracy, IFD top 1 or the flexible selection-based IFD top 2 will give a better correlation than that of rigid docking.[29] In this study, the correlations were typically high for rigid docking and IFD top 2 and moderate for IDF top 1. Moreover, all these five ligands exhibited stronger interactions with the COX-1 enzyme with the average free binding energies

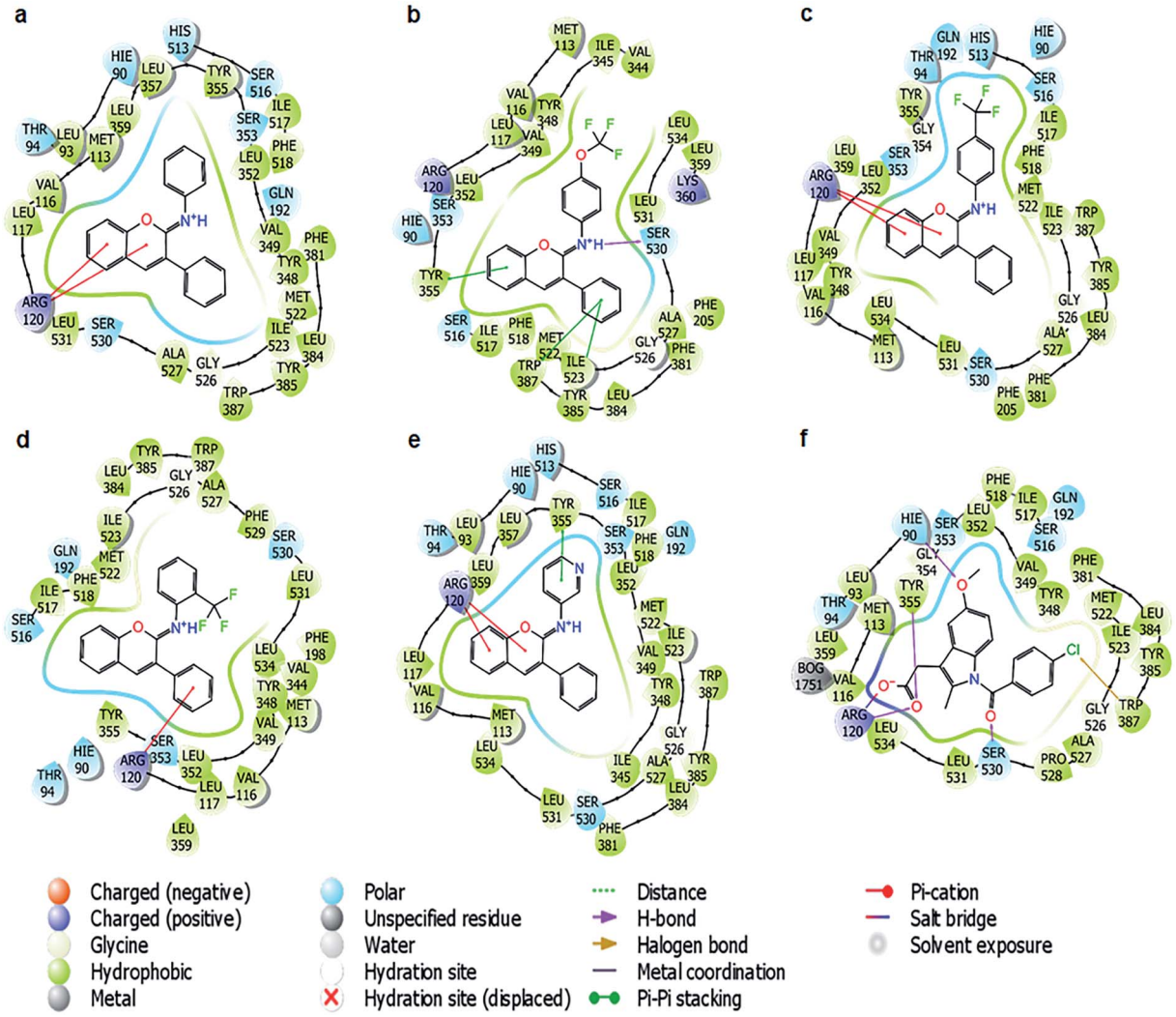


Fig. 4 The binding poses of the five ligands and indomethacin with the cyclooxygenase-1 protein predicted in IFD top 2. (a) Ligand **1**; (b) ligand **10**; (c) ligand **14**; (d) ligand **15**; (e) ligand **20**; (f) standard drug, indomethacin.

of −68.3, −88.1, and −87.4 kcal mol$^{-1}$ using the rigid, IFD top 1, and IFD top 2 methods, respectively, much higher compared to those of indomethacin (−32.3, −76.2, and −55.2 kcal mol$^{-1}$). Obviously, the binding energy calculated by IFD was much stronger than that from rigid docking mostly due to the ability to alter the binding site in IFD to conform with the shape and binding mode of the ligands.

According to the binding poses of the five ligands predicted by IDF top 2, hydrophobic interactions were the main interactions of this congeneric series (Fig. 4). The three aromatic rings chromene, phenyl, and benzenaminium were fused together in these ligands (Fig. 1). They were strongly positioned by π–π stacking with Tyr385, Trp387, Phe518, and/or Tyr348. A marked improvement was recorded when the aromatic electrophile of –$OCF_3$ was substituted at the *para* position of benzenaminium in ligand **10** since anchoring by the –$OCF_3$ group can create many interesting interactions, which were further observed by molecular dynamics (MD) simulation. The Arg120 residue, which is the usual target for H-bond formation in anti-inflammatory drugs, such as indomethacin, was attenuated by π–cation interactions in this congeneric series. The decline inevitably raised questions about the superior inhibitory capacity of these compounds relative to the reference drug and the factors that actually govern its activity.

Similarly, for the COX-2 protein, a good correlation was observed, with the $R^2$ of both IFD top 1 and IFD top 2 at 0.64, while that of rigid docking was stable around 0.52. The mean value of the free binding energy increased by more than 30 kcal mol$^{-1}$ while using the IFD methods. Following a similar trend to COX-1, when these ligands could not form a direct H-bond with the Arg120 residue of the protein, they induced π–π stacking with Tyr385, Trp387 or Tyr355 on one side and gained access to Arg120 on the other side. This binding mode was completely different from that of celecoxib, in which the hydrophobic interactions are overshadowed by three hydrogen bonds with Arg120, Tyr355, and Val116 (Fig. S1†), suggesting a different role of the hydrophobic interactions and hydrogen bonds in the COX-1/2 active sites and the need for dynamic simulation analysis to understand this congeneric series better.

Since the theoretical calculations showed good coherence with the *in vitro* and *in vivo* assays, the ligand-COX-1 complexes were further analyzed using MD simulations to shed light on the inhibitory mechanisms of these compounds on the target proteins.

The first question was whether the π–cation interactions of these ligands with Arg120 were sufficient to inhibit the COX-1 protein? Statistics showed that the π–cation interaction was not a dominant interaction in all these cases. Specifically, only ligand **1** showed a 100% interaction fraction for the π–cation interaction with Arg120, while the rest of the ligands showed rates below 50%, declining in the order of **20** (50%), **14** (40%), **10** (10%), and **15** (0%). In the opposite direction, the hydrophobic interactions, particularly π–π stacking with several aromatic residues, emerged as the substitute for the π–cation interaction of Arg120. From 30% in the case of ligand **1**, these interactions rapidly rose to 50% for ligand **20** and almost 100% for the remaining ligands **14**, **15**, and **10** (Fig. 5 and S2–S5†).

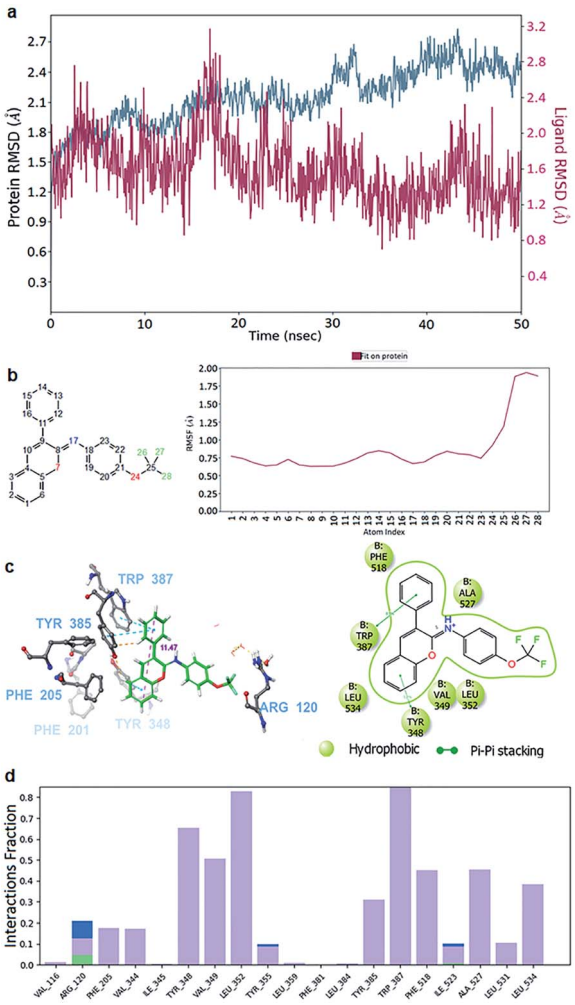


Fig. 5 Molecular dynamics simulation (MDS) of the ligand **10**–cyclooxygenase-1 complex. (a) Root-mean-square deviation of the protein (azure) and ligand **10** (red signal). (b) The root mean square fluctuation (RMSF) of molecule **10** when fitted on the protein (red line). The atom numbers of ligand **10** (left) corresponding to the *X*-axis of the RMSF plot (right). (c) Snapshots 3D (left) from the stable segments of MDS show that ligand **10** formed two π–π stacking interactions with Tyr 385, Trp 387 and Tyr 348 (right). The red dashed line is the measured length between the farthest atoms of the phenyl and chromene groups. The interactions that occur for more than 30.0% of the simulation time in the selected trajectory (0.00 through 50.05 nanoseconds) are shown. (d) Interaction diagram demonstrating the percentage interaction of ligand **10** with the surrounding residues. The red dashed line was the measured length between the farthest atoms of the phenyl and chromene groups.

Meanwhile, the inhibition capacity was also proportional to these π–π stacking interactions. Hence, the next question was whether these interactions really played an essential role even in pairing with Arg120.

The answers could be found at the binding sites of COX-1 and COX-2, which were quite similar to a triangle plane ABC (Fig. 6), in which the AB edge (17 Å in length approximately between –$CH_3$–hydrogen of Met 522 and –CH–hydrogen of ile 345) was the most concentrated place of aromatic residues,

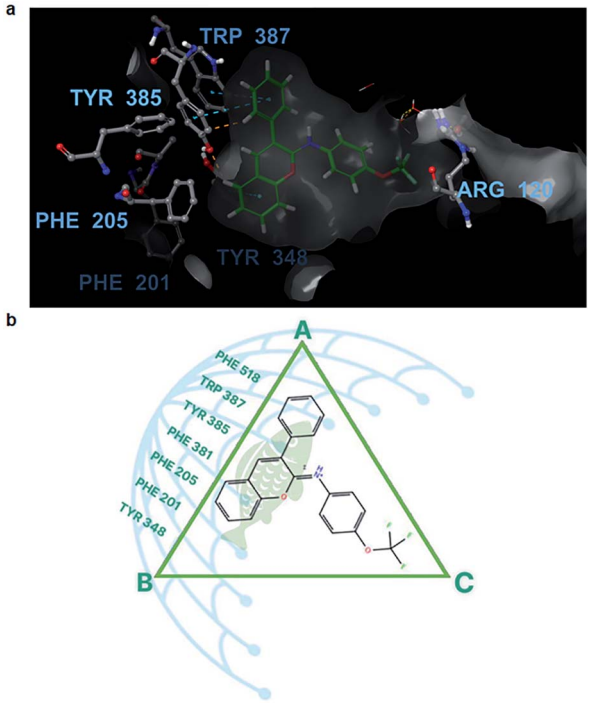


Fig. 6 Ligand **10**–cyclooxygenase-1 (COX-1) interactions. (a) The binding site of COX-1 (grey shape) is inhibited by ligand **10** (green ball and sticks). The surrounding residues are presented as grey balls and sticks. Oxygen is presented in red, nitrogen in blue, carbon in grey, and hydrogen in white. (b) The active site of COX-1 with the distribution of aromatic fused residues on the left side. The fish scales represent the aromatic scaffold of ligand **10**, and each mesh of the fishnet is an aromatic ring that forms a sturdy π–π stacking system on the fish scales.

such as Phe518, Trp387, and Tyr385., and the position of Arg120 was at vertex C of the triangle.

With ligand **10** as the example, the 50 ns molecular dynamic simulation demonstrated many aspects. Firstly, the root-mean-square deviation (RMSD) of ligand **10** was stable under 2.0 Å (Fig. 5a). Next, the chromene or phenyl atoms were the least volatile with the root mean square fluctuation (RMSF) under 1 Å (Fig. 5b). Finally, the hydrophobic interactions due to the π–π stacking of ligand **10** with the aromatic residues Tyr348, Tyr385, Trp387, and Phe518 were all observed over 40% of the interactive time (Fig. 5d). Meanwhile, the length of the chromene frame with the phenyl group was about 12 Å, which perfectly suited their position along the edge AB (Fig. 5c). Therefore, the chromene scaffolds and phenyl groups were squeezed by the π–π stacking interactions with Phe518, Trp387, Tyr385, Phe381, Phe205, Phe201, and/or Tyr348 (Video S1†). Molecules with lengths greater than 12 Å, however, will not be able to produce a drastic reduction in activity because they form bad interactions with the surrounding residues even if they have many polycyclic/bicyclic rings (*i.e.*, compounds **6**, **18**, and **19**). Additionally, a small but worthy contribution was from the interactions of ligand **10** with Arg120. This ligand formed a direct H-bond with Arg120 through the $-OCF_3$ oxygen several ns after the beginning of the simulation, and then it was quickly replaced by hydrophobic interactions or H-bonds *via* water brigdes (Fig. 5c and 6a). Although they only contributed for 20% of the interaction time, ligand **10** was slightly better than the other compounds in terms of free binding energy and presented the best *in vitro* and *in vivo* results of all the tested compounds.

The remaining compounds differed in the distribution of the three principal groups, but they had a common feature in the arrangement such that the number of π–π stacking interactions with the AB edge of the triangle were as high as possible. The MD simulations of the remaining ligands also presented significant hydrophobic interactions at edge AB (Fig. S2–S5 and Videos S2–S5†).

In short, this study has identified a group of NAIs that have potent anti-inflammatory activity and explored the mechanism underlying their inhibitory activity, which was mostly by forming π–cation or π–π stacking interactions with the Arg120 residue. It also demonstrates, for the first time, the role of aromatic moieties in the COX-1 binding site which are as important as the Arg120 residue.

## Experimental methods

### Materials

Twenty-two NAIs (**1–22**) previously synthesized *via* a cross-coupling strategy[26] were used in this study (Fig. 1). Indomethacin and celecoxib were purchased from Sigma Aldrich (USA). All the chemicals used in this study were of analytical grade.

### COX-1/2 inhibitory assays

By using the COX inhibitor screening assay kit (no. 560131, Cayman Chemical Company, MI, USA), the COX-1/2 inhibitory activities of the NAIs were estimated.[30] Indomethacin was used as the reference drug. The test was carried out according to the manufacturer's instructions with some changes. In brief, to 10 μL of the enzyme (COX-1 or COX-2), 10 μL of each test compound solution at four different concentrations (2.5, 5.0, 7.5, 10.0 mg $mL^{-1}$) and 960 μL of a reaction buffer (0.1 M Tris–HCl buffer, pH 8.0, containing 5 mM EDTA and 2 mM phenol) were added. The mixture was incubated at 37 °C for 10 min. Next, 10 μL of 100 μM arachidonic acid (substrate) was added, and the mixture was incubated for 2 min at 37 °C. Afterward, 50 μL of 1 M HCl was added to stop the reaction. The absorbance was spectrophotometrically measured at 410 nm against the blank. This inhibitory assay was performed thrice, and the $IC_{50}$ values were attained *via* logistic regression analysis.

### Animals

Healthy albino rats of both sexes matured between 2-3 months and weighing 180–200 g were procured from the Animal House of Duy Tan University, Vietnam, and fed with the standard pellet diet and water (*ad libitum*) for at least seven days before the study. The experimental protocols were maintained as per the guidelines of the Control and Supervision of Experiments on Animals for experimental clearance by Duy Tan University, Vietnam (code: DTU.2020.934).

### Acute toxicity study

By using the oral acute toxic class method,[27] compound **1** was subjected to an acute toxicity study in healthy male adult albino rats as per the guidelines of the Organization for Economic Co-operation and Development. Compound **1** at 200 mg $kg^{-1}$ b.w was administered orally to five male rats ($n = 5$), and they were examined for physiological and biological changes for 24 h.

### *In vivo* anti-inflammatory activity

By using the formalin-induced hind rat paw oedema assay,[28] the *in vivo* anti-inflammatory activity of the NAIs was estimated. The healthy adult albino rats of both sexes were grouped into thirteen batches containing five adult albino rats ($n = 5$) each. The first batch served as the normal control (dosed only with 0.5% w/v carboxymethyl cellulose (CMC)), while the next two batches were administered with the standard drug indomethacin at 10 and 20 mg $kg^{-1}$ b.w, respectively, and the remaining batches were treated with the five selected compounds (**1**, **10**, **14**, **15**, and **20**) at 10 and 20 mg $kg^{-1}$ b.w. All the test samples were deliquesced in 0.5% w/v CMC and administered intraperitoneally. After 30 min of test sample administration, 0.1 mL of formalin (1% w/v) was administered in the sub-plantar region of the left paw of the rats, while the right paw (non-inflamed) was used as a reference for inflammation. The rat paw oedema volume of all the tested adult albino rats was measured at 1, 2, and 4 h after the test sample dosage using plethysmography. Finally, the measured percentage variation in rat paw oedema (using the below equation) was compared with that caused by indomethacin.

$$\text{Percentage reduction (\%)} = (C - T)/C \times 100$$

in which $C$ is the volume of paw oedema in the control animals, and $T$ is the volume of paw oedema in the treated animals.

### Statistics

The *in vitro* and *in vivo* results are presented as the mean ± SD and mean ± standard error of three and five independent experiments, respectively. The statistical analysis was performed using one-way analysis of variance (ANOVA) followed by Tukey's test for *in vitro* studies and a two-way ANOVA followed by Bonferroni post-tests for *in vivo* studies. The differences were considered statistically significant if $*p < 0.05$ or $**p < 0.01$ or $***p < 0.0001$ when compared to positive control.

### Compound docking and molecular dynamics simulations

*In silico* docking, the MM-GBSA free binding energy evaluations, and rendering the model outputs were executed using the Schrödinger software 2020-3. The correlation scatter plots were generated by Tableau 2020.2. The published crystal structure of the COX-1 (PDB: 3KK6) and COX-2 (PDB: 1CX2) receptors were imported and prepared using the Protein Preparation Wizard[31] (Maestro software, Schrödinger Release 2020-3). Next, the structures of molecules **1–22** and the reference drug indomethacin were created and prepared by Ligprep.[32] The general process of standard precision (SP), extra precision (XP) docking and molecular mechanics/generalized born surface area (MM-GBSA) free binding energy estimation have been previously described.[31] Notably, the Ligand Filtering operation was performed to refine all ligands using the SP method with Glide-score $\leq -8.5$ kcal $mol^{-1}$ before proceeding with XP docking. An induced fit docking (IFD) protocol[33–35] was used in tandem with the Glide SP, XP dockings to predict the accurate complex structures of the ligand and proteins. From there, the system set-up for molecular dynamics simulations for docked ligands was built with COX-1 and COX-2 by using Desmond[i]. The general conditions of Desmond were established according to the previous study.[36] The solvent model was set with a flexible simple point-charge water model with the OPLS3e force field. 50 nanoseconds (ns) and 50 picoseconds (ps) were set as the total simulation time and the trajectory recording interval, respectively. The temperature was 300.0 K, and the pressure was 1.01325 bar, while the Relax model system was the default option. The experimental binding energies ($\Delta G_{exp}$) were calculated using the equation $\Delta G_{exp} = -RT \ln IC_{50}$, where the gas constant $R = 1.987$ cal $mol^{-1}$ $K^{-1}$ and the temperature $T = 300$ K.

## Conclusions

Twenty-two previously synthesized NAIs were screened for their anti-inflammatory activity by performing an *in vitro* anti-inflammatory assay against COX-1/2 enzymes. Five compounds (**1**, **10**, **14**, **15**, and **20**) that gave the best *in vitro* anti-inflammatory results were subjected to an *in vivo* anti-inflammatory assay using the formalin-induced hind rat paw oedema method, followed by *in silico* studies using indomethacin as the standard drug. Among these, compound **10** exhibited an outstanding anti-inflammatory property in all the *in vitro*, *in vivo* and *in silico* studies. This achievement was due to the excellent suitability of the chromene-phenyl scaffold with a highly concentrated nucleated area of aromatic residues, which produced good π–π stacking interactions. The results of this study show that compound **10** is a potent anti-inflammatory agent that can be considered as a candidate for anti-inflammatory drug research.

## Funding

This study was supported by the Department of Science and Technology (India) for the research grant, BRICS (Grant no. DST/ICP-BIO/1798) for the research funding. The funders had no role in study design, data collection and analysis, decision to publish, or preparation of the manuscript.

## Ethical statement

The animal experiments were performed in accordance with the guidelines of Control and Supervision of Experiments on Animals and approved by the ethics committee at the Duy Tan University, Vietnam (code: DTU.2020.934).

## Author contributions

HTN and VBT designed and conducted the *in vitro* and *in vivo* experiments and data analysis and co-wrote the manuscript. T-YV, VNHH, and PTNM designed and conducted the *in silico* experiments and data analysis. VKA and PSM synthesized the chemical compounds.

## Conflicts of interest

There are no conflicts to declare.

## Acknowledgements

The authors would like to thank Mr Toai Tuyn Phan (a technical staff, the High Potential Computer group, Ton Duc Thang University) and Dr Duc Duy Vo (Uppsala University, Sweden) for their supports.

## References

1 M. Y. Huang, J. Lin, Z. J. Huang, H. G. Xu, J. Hong, P. H. Sun, J. L. Guo and W. M. Chen, *Medchemcomm*, 2016, **7**, 658–666.
2 L. Ferrero-Miliani, O. H. Nielsen, P. S. Andersen and S. E. Girardin, *Clin. Exp. Immunol.*, 2007, **147**, 227–235.
3 L. Z. Chen, W. W. Sun, L. Bo, J. Q. Wang, C. Xiu, W. J. Tang, J. B. Shi, H. P. Zhou and X. H. Liu, *Eur. J. Med. Chem.*, 2017, **138**, 170–181.
4 X. Y. Lu, Z. C. Wang, S. Z. Ren, F. Q. Shen, R. J. Man and H. L. Zhu, *Bioorg. Med. Chem. Lett.*, 2016, **26**, 3491–3498.
5 P. Libby, *Nature*, 2002, **420**, 868–874.
6 H. Y. Kim, H. V. Kim, S. Jo, C. J. Lee, S. Y. Choi, D. J. Kim and Y. Kim, *Nat. Commun.*, 2015, **6**, 1–14.
7 C. Rommel, M. Camps and H. Ji, *Nat. Rev. Immunol.*, 2007, **7**, 191–201.
8 C. A. Velázquez, Q. H. Chen, M. L. Citro, L. K. Keefer and E. E. Knaus, *J. Med. Chem.*, 2008, **51**, 1954–1961.
9 S. Lucas, *Headache*, 2016, **56**, 436–446.
10 M. P. Draper, R. L. Martell and S. B. Levy, *Br. J. Cancer*, 1997, **75**, 810–815.
11 G. A. FitzGerald and C. Patrono, *N. Engl. J. Med.*, 2001, **345**, 433–442.
12 K. D. Rainsford, *Am. J. Med.*, 1999, **107**, 27–35.
13 K. D. Rainsford, *Subcell. Biochem.*, 2007, **42**, 3–27.
14 G. A. FitzGerald, *N. Engl. J. Med.*, 2004, **351**, 1709–1711.
15 J. Jacob P, S. L. Manju, K. R. Ethiraj and G. Elias, *Eur. J. Pharm. Sci.*, 2018, **121**, 356–381.
16 J. Bost, A. Maroon and J. Maroon, *Surg. Neurol. Int.*, 2010, **1**, 80.
17 N. Sultana and Z. Saeed Saify, *Anti-Inflammatory Anti-Allergy Agents Med. Chem.*, 2012, **11**, 3–19.
18 M. B. Palkar, A. S. Singhai, P. M. Ronad, A. H. M. Vishwanathswamy, T. S. Boreddy, V. P. Veerapur, M. S. Shaikh, R. A. Rane and R. Karpoormath, *Bioorg. Med. Chem.*, 2014, **22**, 2855–2866.
19 S. A. Patil, S. A. Patil and R. Patil, *Future Med. Chem.*, 2015, **7**, 893–909.
20 D. Kashyap, A. Sharma, H. S. Tuli, S. Punia and A. K. Sharma, *Recent Pat. Inflammation Allergy Drug Discovery*, 2016, **10**, 21–33.
21 M. Costa, T. A. Dias, A. Brito and F. Proença, *Eur. J. Med. Chem.*, 2016, **123**, 487–507.
22 P. Proksch and E. Rodriguez, *Phytochemistry*, 1983, **22**, 2335–2348.
23 I. E. Bylov, M. V. Vasylyev and Y. V. Bilokin, *Eur. J. Med. Chem.*, 1999, **34**, 997–1001.
24 J. Grover and S. M. Jachak, *RSC Adv.*, 2015, **5**, 38892–38905.
25 H. M. Revankar, S. N. A. Bukhari, G. B. Kumar and H. L. Qin, *Bioorg. Chem.*, 2017, **71**, 146–159.
26 P. S. Mandal and A. V. Kumar, *Synlett*, 2016, **27**, 1408–1412.
27 V. B. Tatipamula, M. K. Kolli, S. B. Lagu, K. R. Paidi, P. R. Reddy and R. P. Yejella, *Pharmacol. Rep.*, 2019, **71**, 233–242.
28 V. B. Tatipamula and G. S. Vedula, *Nat. Prod. J.*, 2020, **10**, 87–93.
29 E. B. Miller, R. B. Murphy, D. Sindhikara, K. W. Borrelli, M. J. Grisewood, F. Ranalli, S. L. Dixon, S. Jerome, N. A. Boyles, T. Day, P. Ghanakota, S. Mondal, S. B. Rafi, D. M. Troast, R. Abel and R. A. Friesner, *J. Chem. Theory Comput.*, 2021, **17**, 2630–2639.
30 H. T. Nguyen, T.-Y. Vu, V. Chandi, H. Polimati and V. B. Tatipamula, *Sci. Rep.*, 2020, **10**, 15965.
31 J. Li, R. Abel, K. Zhu, Y. Cao, S. Zhao and R. A. Friesner, *Proteins: Struct., Funct., Bioinf.*, 2011, **79**, 2794–2812.
32 G. M. Sastry, M. Adzhigirey, T. Day, R. Annabhimoju and W. Sherman, *J. Comput.-Aided Mol. Des.*, 2013, **27**, 221–234.
33 R. Farid, T. Day, R. A. Friesner and R. A. Pearlstein, *Bioorg. Med. Chem.*, 2006, **14**, 3160–3173.
34 W. Sherman, H. S. Beard and R. Farid, *Chem. Biol. Drug Des.*, 2006, **67**, 83–84.
35 W. Sherman, T. Day, M. P. Jacobson, R. A. Friesner and R. Farid, *J. Med. Chem.*, 2006, **49**, 534–553.
36 T. V. Pham, H. N. T. Hoang, H. T. Nguyen, H. M. Nguyen, C. T. Huynh, T. Y. Vu, A. T. Do, N. H. Nguyen and B. H. Do, *BioMed Res. Int.*, 2021, **2021**, 1–10.